Optimizing Arsenic Removal in a Groundwater Treatment Cell

Luke Russell

A report prepared in partial fulfillment of
the requirements for the degree of

Master of Science
Earth and Space Sciences: Applied Geosciences

University of Washington

January 2020

Project mentors:
Adriana Jarosz
Michelle Myers

Internship coordinator:
Kathy Troost

Reading committee:
Michael Brown
Drew Gorman-Lewis

MESSAGe Technical Report Number: 088

Table of Contents

Executive Summary

The goal of this research is to investigate geochemical factors on arsenic removal from groundwater in a groundwater treatment cell. The treatment cell is near Metaline Falls, WA, and is operated by Geosyntec Consultants. Using PHREEQ-C, a program developed by the USGS for chemical modeling, I determined which adsorptive media will remove the most arsenic under site conditions, which ions inhibit or encourage arsenic adsorption, and which ions have the potential to remove arsenic through co-precipitation.

The groundwater samples collected from the site were taken to the UW SEFS Analytical Lab for inductively coupled plasma mass spectrometry (ICP-MS) to determine the concentrations of each ion present in the groundwater. These lab results were used for the model validation initial conditions. Historical data collected at the site by Geosyntec was compiled into a database for statistical analysis, which identified conductivity, a proxy for ionic strength, and manganese in solution as two main factors influencing arsenic removal. These factors were further studied using PHREEQ-C.

From the modeling results I found that titanium oxide media, particularly MetasorbG manufactured by Graver Technologies, to be the most efficient media at removing arsenic via adsorption. I found that phosphate in the groundwater plays the largest role in inhibiting arsenic adsorption by directly competing with arsenate for surface sites. Conductivity, or ionic strength, will reduce adsorption rates upgradient of the treatment cell and lead to higher arsenic concentrations being delivered to the cell. And, finally, I determined that arsenic is oxidized by manganese oxides and will readily precipitate with manganese ions in high pH conditions, which are typically found upgradient of the treatment cell.

For further study, I recommend monitoring phosphate levels in the treatment cell, determining residence time of the water in the treatment cell, performing XRD or FTIR analysis on gravel inside the treatment cell to determine what minerals are precipitating, and starting two batch-scale trials with titanium oxide and manganese oxide media.

1.0 Introduction

This project investigates adsorptive filter media and associated favorable geochemical conditions for increasing arsenic removal in groundwater impacted by a closed cement kiln dust (CKD) landfill. This project will support Geosyntec Consultants' (Geosyntec) ongoing work by evaluating the potential addition of an adsorptive media filtration treatment step to the existing treatment system. I evaluated four solid media that could be implemented within the treatment cell. We selected the adsorptive media based on appropriateness of the media application and availabity of surface complexation literature with arsenic reactions. The alternative media include AAFS50 (activated alumina) and MetasorbG (titania-based media). This report relies on a surface complexation model to determine the ideal geochemical conditions for arsenic removal for the selected media using PHREEQC (pH-Redox-Equilibrium) software. The advantage of using a surface complexation model over an empircally derived model, such as the Langmuir and Fruendlich isotherm models, is that the methodology is not site-specific and can be applied to any treatment site with only a simple water ion analysis.

The significance of this work is to decrease the concentrations of arsenic in groundwater. Arsenic is a common contaminant found in groundwater with both natural and industrial sources. Exposure to high levels of arsenic can cause illness, such as nausea, vomiting, damage to blood vessels, cancer, and even death (EPA 2000). Removal of arsenic from the environment is required for both ecological and public health reasons (Bowell et al., 2014; EPA, 2000). Potential fish impacts in downgradient Sullivan Creek via offsite groundwater flow pose the primary toxicity concern at this site.

2.0 Background

2.1 Site History

The project site is an active remediation site located in Metaline Falls, Washington (Figure 1). A closed CKD (closed cement kiln dust)landfill has historically caused site groundwater pH to become highly basic. Cement kiln dust is the fine-grained, alkaline byproduct of cement production. The increase in pH has mobilized arsenic, in the form of arsenite and arsenate, into the groundwater. The landfill has been capped to inhibit additional leaching (Figure 2). Groundwater is now diverted into a treatment cell prior to discharge into downgradient Sullivan Creek (Geosyntec, 2006).

Before construction of the treatment cell in 2006, groundwater arsenic concentrations at the site have been as high as 750 milligrams per liter (mg/L). The site is currently being remediated in cooperation with the Washington Department of Ecology (Ecology). Ecology has established the current maximum contaminant level for arsenic cleanup in groundwater as 5 micrograms per liter (µg/L), although this may be revised during the upcoming permit cycle. Since construction of the treatment cell, arsenic levels at the site have fluctuated between 0 and 50 µg/L. Geosyntec presently incorporates carbon dioxide (CO_2) diffusion and groundwater recirculation/aeration technologies within the treatment cell to neutralize pH and stimulate metal/metalloid (including arsenic) precipitation reactions (Figure 4). Although the treatment cell has been effective at removing arsenic from groundwater, the data collected during this project will assist Geosyntec in improving and optimizing arsenic removal.

2.2 Geologic and Hydrologic Setting

Metaline Falls is on the Pend Orielle River in the Selkirk Mountain Range. The CKD landfill is on a river terrace of glaciofluvial and glaciolacustrine sediment. The glacial sediments are predominantly sandy silt and clayey silt, and are subject to landsliding. Evidence of a dormant landslide is apparent immediately to the south of the closed CKD pile (Figure 1). At the site, glacial sediment is covered by Holocene alluvium from Sullivan Creek, with a few ravines incised into the glacial sediment. This 20 foot thick layer of alluvium is mostly gravel with occasional cobbles and boulders and intersperesed layers of sand, silt, and clay (Geosyntec, 2006).

Sullivan Creek, which is fed by Lake Sullivan, has a watershed of 90,880 acres and a mean flow between 100 and 650 cfs. The highest flows are recorded in May and June during snowmelt, while the lowest flows occur during August and September. Sullivan Creek flows into the Pend Orielle River less than a mile downstream of the treatment cell and the closed CKD pile. Groundwater at the site generally flows north and east under the closed CKD pile into Sullivan Creek through the Holocene alluvium and sand lenses intersperesed in the glacial sediment. Depth to groundwater ranges from 2-3 feet in the floodplain (near Sullivan Creek) and increases to 5-6 feet at the toe of closed CKD pile (Geosyntec, 2006).

2.3 Surface Charge

The overall charge of a mineral surface can be broken apart into three types: permanent, coordinative, and dissociative charge (Davies and Kent, 1990). Permanent charge is from substitions of elements within the mineral structure, such as Al^{3+} replacing Si^{4+} in silicate oxides. The permanent charge of a mineral may be positive or negative, but is more commonly negative. Coordinative charge is determined by reactions between ions in solution and surface function groups. These reactions commonly bind, or adsorb, ions of opposite charge of the permanent charge in a layer on the mineral surface. Because the permanent and cooridnative charge does not always net zero charge, and third type of surface charge is necessary to desribe the mineral-solution interface. The dissociative charge is made up of the accumualtion of ions in solution that form a diffuse atmosphere around the mineral surface and compact layer of cooridnative bonds.

In order to understand how arsenic bonds to surfaces and how surface charge is modeled in this report I present a brief history of the electrical double layer. A German physiscist named Hermann von Helmholtz first postulated that counterions (ions of the opposite charge of the surface) bind to a charged surface to form a compact layer with constant differential capacitance or charge across the layer. This was the beginning of a concept known as the electrical double layer. Sixty years later, French physicist Louis Georges Gouy and English physicist David Leonard Chapman described the mineral-solution interface as a diffuse layer of counterions where the charge decayed exponentially with distance from the surface. The

Guoy-Chapman theory is able to account for mixing of ions in the solution with the surface and variable surface charge due to solution parameters such as pH and ionic strength where the Helmholtz theory could not. A decade later in 1924, a German-American physicist named Otto Stern modified the Gouy-Chapman theory, which often overpredicted charge close to the mineral surface, by accounting for the fact that ions can only approach the surface within some finite distance that corresponds to the ionic radius of the counterion. Stern's approach to modeling surface charge became known as the Gouy-Chapman-Stern theory, as it combined the ideas of Helmholtz, Guoy, and Chapman into a single model. A simplified depiction of all three models (Helmholtz, Gouy-Chapman, and Stern) can be seen in Figure 5, which is taken from Wu and Qiao (2014). The Gouy-Chapman-Stern theory, also known as the diffuse double layer model, is the foundation of the surface complexation modeling done in this report. Arsenic is capable of bonding to surfaces through outer-sphere complexes in the diffuse layer, and inner-sphere complexes within the compact Helmholtz layer.

2.4 Arsenic Speciation and Adsorption

Arsenic occurs in our in environment in two main water-soluble forms: arsenite (AsO_3^{-3}) and arsenate (AsO_4^{-3}). Both arsenic species are anions capable of adsorbing to mineral surfaces. However, arsenate, the species with higher oxidation state, is more reactive than arsenite, and it is often necessary to convert arsenite to arsenate through some method of oxidation to yield effective adsorption rates (Bowell et al. 2014). Because arsenic adsorption is so dependent on chemical conditons such as pH, it is assumed that arsenic mostly interacts with charged surfaces as a counterion in the diffuse layer. Arsenic ions, and most anions, will not react with a mineral surface until the pH of the solution has dropped below the point-of-zero-chargeor pH_{ZC}. The pH_{ZC} is the pH at which the mineral surface exhibits a net zero charge in the absence of all other ions besides protons and hydroxide (Figure 12). This is the pH where the surface functional groups protonate or deprotonate, and is similar to the pKa of a reaction. For a negatively charged surface, protons make up the majority of the Helmholtz/Stern layer at pHs below the pH_{ZC}, allowing for arsenic anions to adsorb to the mineral surface in the diffuse layer. Therefore, for the

effective remediation of arsenic it is necessary to oxidize arsenite into arsenate, and reduce the pH to below the pH_{ZC}.

2.4 Surface Complexation Modeling

To understand the chemical mechanics that affect arsenic removal, I used surface complexation modeling. Surface complexation models (SCMs) attempt to predict chemical equilibrium by using adsorption equilibrium constants and surface characteristics (site density and specific surface area). Surface complexation modeling relies on balancing reactions between the adsorbent and surface functional groups as well as electrostatics and thermodynamics to determine adsorption. SCMs differ from non-electrostatic models that rely on the creation of isotherms to determine adsorption for a given surface. Adsorption isotherms such as the Langmuir and Fruendlich isotherms are created by comparing equilibrium concentrations of adsorbent to initial concentrations for a given amount of adsorbate. This empirical approach can often predict adsorption for given surfaces and site conditions more accurately than surface complexation modeling, but it does not provide insight into which chemical species and reactions are playing a key role.

Many SCMs have been created to describe the adsorption of arsenic onto various minerals and synthesized adsorption media (Goldberg, 1986; Dzombak and Morel, 1990; Han et al., 2010; Kanematsu et al., 2013; Pena et al., 2006; Su et al., 2008; Sverjensky and Fukushi, 2006). Different SCMs include the constant capacitance, the double layer, and the triple layer models, which are all various takes on the electrical double layer described in section 2.3. The SCM I used in this report is commonly known as the diffuse double layer model (or Gouy-Chapman-Stern model). I chose to use a diffuse double layer for this report despite evidence of triple layer models yielding more accurate results for arsenic adsorption (Sverjensky and Fukushi, 2006) largely due to the wide availability of diffuse double layer SCMs in literature and the capabilities of PHREEQ-C.

3.0 Methods

3.1 Field Work

In order to properly model in-situ conditions in PHREEQ-C, it is necessary to get an accurate assessment of all of the ions present in the groundwater. Geosyntec has monitored the site for certain ions of concern, such as lead, chromium, manganese, and arsenic, but there has not been a thorough groundwater ion assessment since the design report in the 2006. The main goal of the field work was to collect groundwater samples to determine the concentrations of all the ions present both in the treatment cell and in the groundwater up-gradient of the treatment cell.

I collected field groundwater samples with a sump pump to draw water from the wells. The samples come from two outlet wells (TZ-01 and TZ-03), the recirculation system within the treatment cell, and three wells up-gradient of the treatment cell (MW-09, PM-01, PM-05) (Figure 3). I chose these wells in order to get an idea of the spatial variation of chemical parameters and ion concentrations at the site and to compare geochemical conditions upgradient of the treatment cell to conditions within the cell. The groundwater samples were collected in 50 mL polypropylene vials. Headspace was minimized to prevent oxidation of the sample, and the samples were put directly on ice to be transported to the lab the following day. While collecting the groundwater samples, I used a Horiba water quality meter to measure in-situ water quality data; these data can be found in Table 3. These parameters such as pH and temperature are useful inputs for PHREEQ-C to best represent actual site conditions. The University of Washington, School of Environmental and Forest Sciences Analytical Lab provided inductively coupled plasma-mass spectrometry (ICP-MS) analysis to determine the concentrations of ions and species in the samples; these results are reported in the appendix (Section 10.4).

3.2 Modeling

I compiled a database of arsenic surface complexation for two different media used commonly in heavy metal remediation projects: titania oxide (Pena et al., 2006) and activated alumina (Su et al., 2008).

The arsenic surface complexation database builds onto the minteq.v4 database (developed and maintained by the USGS) for this project; this database already contains the surface complexation reactions for arsenic and hydrous ferric oxide (Hfo). The additions to the minteq database for use in PHREEQ-C can be found in the appendix (Section 10.2). I created a geochemical model in PHREEQ-C using the arsenic-media complexation database and ion concentrations determined from the ICP-MS analysis.

All model trials were run using 1 ppm (or 1000 ppb) arsenic, and 0.09 grams of solid media. I chose to use 1 ppm of arsenic, a value two orders of magnitude higher than arsenic concentrations commonly reported at the site, in all of my models because the purpose was to investigate the mechanics that encourage or inhibit arsenic removal under the given site conditions- not to create a model of true site conditions. Using low arsenic concentrations of 1 – 50 ppb in the model made it difficult to see effects of different ions on arsenic adsorption, as most, if not all, of the arsenic was adsorbed regardless of the other ions present in the model. I chose to use 0.09 grams of media in my modeling because it is the default amount used in the surface complexation example in the PHREEQ-C documentation (Parkhurst and Appelo, 2013). More importantly, I chose to use 0.09 grams of media in my model because PHREEQ-C runs all simulations with one kilogram of solution, so choosing an amount of media orders of magnitude smaller than the amount of solution accounts for the need of the media to have a long lifespan of effectiveness.

To validate the model, I ran a trial comparing the measured concentrations of ions and species present in the outlet of the treatment cell to the model prediction of final concentrations after the CO_2 treatment (Figure 6). The inputs for the validation trial come from the lab results of the wells up-gradient of the treatment cell (Table 2), which represent the untreated groundwater. The model results are compared to the lab results of the samples from within the treatment cell (Appendix 10.3). The model is not an exact match to what was measured in reality for two primary reasons. First, the input concentrations I used were an average of three upgradient wells and this does not account for all the possible inputs of groundwater into the treatment cell. This is likely why the levels of calcium and iron measured in the treatment cell do not match what was predicted by the model. Second, PHREEQ-C

predicts chemical equilibrium, and it is likely that conditions inside the treatment cell never reach equilibrium or are still equilibrating. Therefore, the phosphorous levels predicted by the model are lower than the measured levels, because adsorption is still occurring.

To investigate the efficacy of different media, I ran trials with only arsenic and the media. While this is not representative of in-situ conditions, it reflects the current information available for surface complexation of industry media. For example, the equilibrium constants for the adsorption of phosphate onto AAFS50 have not been studied (or are not available for this study) so the model would not accurately reflect the inhibition of arsenic adsorption on activated alumina. Similarly, for investigating the effects of various ions on arsenic adsorption, model trials were run using only arsenic and the ion in question. This makes it easier to see the relationship between arsenic, the media, and each ion, but does not account for other reactions that may occur between the ion and other ions/species present in the solution.

3.3 Determining Factors Influencing Arsenic Removal from Historical Data

In order to determine other factors that may be influencing arsenic removal at the site that was not apparent from the surface complexation modeling, I analyzed historical data of site conditions provided by Geosyntec. Measurements of pH, conductivity, turbidity, dissolved oxygen, temperature, oxidation-reduction potential, and other toxic heavy metal concentrations (lead, chromium, and manganese) were compared to arsenic concentration. Twenty years of field and lab measurements were analyzed, combining two databases and filtering out duplicates and entries that do not have all the parameters listed above available. I used the Pearson correlation coefficient, calculated by the covariance of each parameter with arsenic concentration normalized by the product of their standard deviations, to determine which variables with strong influence over arsenic concentration would be worth further investigation in PHREEQ-C. From the calculated Pearson values (Table 1) along with scatterplots of each parameter with arsenic concentration, I determined the two parameters to further investigate through PHREEQ-C were conductivity, a proxy for ionic strength, and manganese concentration. The python script used to filter the

data and create the correlation coefficient matrix can be found in Table 1, and the filtered database is available in the supplemental information.

4.0 Results

4.1 Comparing Effects of Different Media on Arsenic Adsorption

For this report I compared the effectiveness of two media commonly used in environmental remediation: titania oxide and activated alumina to remove arsenic from solution via adsorption. Titania oxide (TiO_2) is a common adsorption media used for remediation of inorganic metals. The synthetic titania oxide media used in this model is MetasorbG from Graver Technologies. Activated alumina (Al_2O_3), another common adsorption media, is modeled using the synthetic media AAFS50, from Axens Solutions. I compared each of these media to the effectiveness of hydrous ferric oxide (Hfo) to adsorb arsenic because I assume that Hfo is the predominate precipitate currently in the treatment cell that is readily adsorbing arsenic. I make this assumption for three reasons: Hfo is one of the most common naturally occurring precipitates in natural systems, surface complexation with Hfo is extremely well documented by the minteq database in PHREEQ-C, and I saw evidence for an abundance of iron precipitates (i.e. orange/rust staining covering gravel in the recirculation system) during my visit to the site.

Figure 7 shows the comparison of titania oxide and activated alumina to Hfo under simple conditions, meaning the only ions present in the simulation were arsenic. The media could not be compared to Hfo under more complex conditions because of the lack of surface complexation data for synthetic media with other ions besides arsenic.

For Hfo arsenic adsorption begins around a pH of 11 and reaches maximum adsorption at a pH of 8. Titania oxide will adsorb arsenic at slightly higher pH values than hydrous ferric oxide, with adsorption beginning at a pH of 11, and reaching maximum at a pH of 9. While activated alumina showed some adsorption of arsenic at pH values greater than 12, the maximum adsorption did not occur until a pH of 5.

4.2 Comparing Effects of Different Ions on Arsenic Adsorption

Similarly to the comparison of effects on arsenic adsorption of different media, I compare the effects of different ions of arsenic adsorption using simple solutions that only contain Hfo, arsenic, and the ion. While PHREEQ-C and the minteq database can model the cumulative effects of all present ions at once (Figure 9), I wanted to isolate the effects of each ion. For effects on arsenic adsorption I focus on four ions: magnesium, calcium, phosphate, and sulphate. Manganese is discussed separately, as its affects on arsenic removal are primarily through coprecipitation, not adsorption.

Calcium and magnesium both encourage the adsorption of arsenate at higher pH values by effectively lowering the surface charge of hydrous ferric oxide (Azam et al. 2010). Figure 8 shows Ca^{2+} and Mg^{2+} ions have a high affinity for hydrous ferric oxide at pH values above the pH_{ZC} when the surface is negatively charged from hydroxyl groups. When these cations bond to the surface they reduce the net-negative charge of the surface, which in turn is more attractive to the negatively charged arsenate (AsO_4^{-3}) ions. However, below a pH of 8 the surface does not hold a strong enough negative charge to attract cations, and the calcium and magnesium no longer help mitigate the negative surface charge.

As shown in figure 8, phosphate and sulfate discourage the precipitation of arsenic by competing for the adsorption sites at lower pH values. This finding is supported by previous studies such as Wilkie and Hering, 1996. Unlike cations such as calcium and magnesium that make the surface more positively charged, anions like sulfate (SO_4^{2-}) and phosphate (PO_3^{3-}) make the surface more negatively charged and less likely to attract arsenate. Sulfate does not begin adsorbing until the pH is below 6, while phosphate adsorbs in a pH range of 6.5 to 9.5. Phosphate is likely the largest inhibitor to arsenic adsorption due to its preferred pH range of adsorbance aligning with the target pH range inside the treatment cell.

Unlike the ions discussed above, manganese does not interact with the Hfo surface. According to the PHREEQ-C model, at pH values greater than 5.5 manganese precipitates as a variety of manganese oxides. Adsorption of arsenic to these manganese oxides is likely to occur, but is not accounted for in the

model. The primary manganese oxides are birnessite, pyrolusite, nsutite, bixbyite, and manganite. From modeling site conditions in PHREEQ-C I found at pH greater than 9, krautite and other hydrated manganese-arsenate minerals, will readily precipitate. Manganese is known to oxidize arsenic from As(III) to As(V) via a two-step pathway (Tournassat et al., 2002). The end result is the formation of arsenate and reduced Mn(II), which are both required for the precipitation of krautite.

Figure 9 shows the cumulative effects of all the ions in one simulation, which is compared to the simple solution of just arsenic and Hfo. The cumulative effects of all the studied ions lead to an increase in arsenic adsorption at pH values above the pH_{ZC} for Hfo (pH_{ZC} = 8.1) and reduced adsorption at pH below the pH_{ZC}.

4.3 Effect of Ionic Strength on Arsenic Adsorption

Because the Pearson values of the historical data found conductivity, a proxy for ionic strength, to be a higher predictor of arsenic concentrations than oxidation-reduction potential and pH, I modeled different ionic strength conditions in PHREEQ-C. While higher ionic strength indicates there are more ions present in the solution (including arsenic), I wanted to determine if there were any inhibitory effects.

Figure 11 shows the effects of ionic strength on arsenic adsorption for a simple solution of Hfo and arsenic. Sodium and chlorine were added for the high ionic strength simulation, because they do not interact with the Hfo surface or arsenic but still raise the ionic strength. Adsorption of arsenic is inhibited most notably at values above the pH_{ZC} of Hfo. While higher conductivity means there is likely higher levels of arsenic to begin with, there is also an increased delivery of arsenic to the treatment cell due to the inhibitory affects of high ionic strength at pH levels above the pH_{ZC}, which is commonly reported upgradient of the treatment cell.

5.0 Discussion

There are a variety of geochemical factors that influence the removal of arsenic from groundwater. Based on the surface complexation modeling in this report the factors that inhibit the removal of arsenic from the groundwater the most are high ionic strength of the groundwater and high phosphate levels, both of which reduce adsorption rates. Factors that encourage the removal of arsenic the

most are the presence of calcium and magnesium via increasing adsorption, and coprecipitation of arsenic with manganese.

It is possible that during times of high conductivity (a proxy for ionic strength) in the groundwater, the charge of the surface layer becomes strong enough to effectively block surface sites by repelling ions in the diffuse layer- drastically reducing the available surface area for adsorption (Dai et al. 2016; Zhang et al. 2019). Therefore, a stronger charge due to higher ionic strength of the surface layer will inhibit both inner-sphere and outer-sphere complexes of arsenic with the surface (Figure 11).

The presence of high levels of manganese is concurrent with very low levels of arsenic, and vice versa (Figure 12). It is likely that the presence of manganese encourages the oxidation of arsenic, the precipitation of a manganese-arsenic mineral (krautite), and the creation of more mineral surface available for adsorption upgradient of the treatment cell.

Because surface complexation models are only as accurate as the studies that determine the surface characteristics and reaction constants, the SCM in this study is largely dependent on the referenced literature. Because of this lack of supporting literature, the model cannot accurately predict how arsenic will adsorb to titania oxide and activated alumina with ions such as calcium, magnesium, or phosphate present. Most literature does not report the reactions of arsenite with media surfaces due to the adsorbance of arsenite often being negligible. Therefore, my model inputs elemental arsenic and allows PHREEQ-C to speciate arsenic depending on the solution conditions, and only the arsenic in the form of arsenate is adsorbed. The SCM in this study was only validated using input parameters from a single day during my field visit (late summer), and does not represent the wide variety of possible geochemical conditions present at the site. PHREEQ-C also reports equilibrium conditions and concentrations, and it is very likely that conditions inside the treatment cell and upgradient never have the time required to reach equilibrium, especially in the spring months when high groundwater volumes from snowmelt flush the system.

6.0 Conclusion

Based on each media's ability to adsorb arsenic in low ionic strength conditions with no other ions present, titania oxide (MetasorbG) is the best media to use for arsenic removal. The presence of calcium and magnesium ions will encourage arsenic removal at high pH values, reducing the negative surface charge. Phosphate and sulfate will discourage arsenic removal by competing for sites and reducing the positive charge on the surface in a low-to-mid pH range. Ionic strength of the solution plays a large role in the adsorption of arsenic, but unfortunately there are no effective and minimally invasive ways to lower the ionic strength of groundwater on a large scale.

My recommendations for further study and next steps include monitoring phosphate and sulfate levels both in the treatment cell and upgradient, determining seasonal residence time of water inside the treatment cell, excavating gravel from inside the treatment cell to determine the composition of precipitates, and starting batch scale trials with titanium oxides and manganese oxides.

From this study phosphate and sulphate have been shown to inhibit arsenic adsorption at the site, but it is unknown if high phosphate levels in the groundwater are a chronic problem or a one-off result of me sampling the groundwater when there happened to be high levels of phosphate and sulfate.

Because PHREEQ-C reports conditions at equilibrium and not the time it takes to reach said equilibrium, determining the residence time of water inside the treatment cell and starting batch-scale trials with media that have proved to be effective at removing arsenic, titanium oxide and manganese oxide media, would be necessary to determine whether the use of this media would be feasible on a large scale. This would answer questions such as, how much media is required, how often would it have to be replaced, and how long does the water have to be in contact with the media for effective removal of arsenic.

Finally, an analysis of the gravel currently in the treatment cell would give insight into the iron and manganese minerals that are precipitating and creating the surfaces for arsenic to adsorb to.

Manganese oxides have been shown to not only remove arsenate, but also oxidize arsenite (Zhang et al., 2014; Tournassat, 2002). This would lead to more accurate modeling and a better understanding between the relationship between manganese and arsenic within the treatment cell, which is likely the key to maintaining arsenic levels below the MCL.

8.0 Figures and Tables

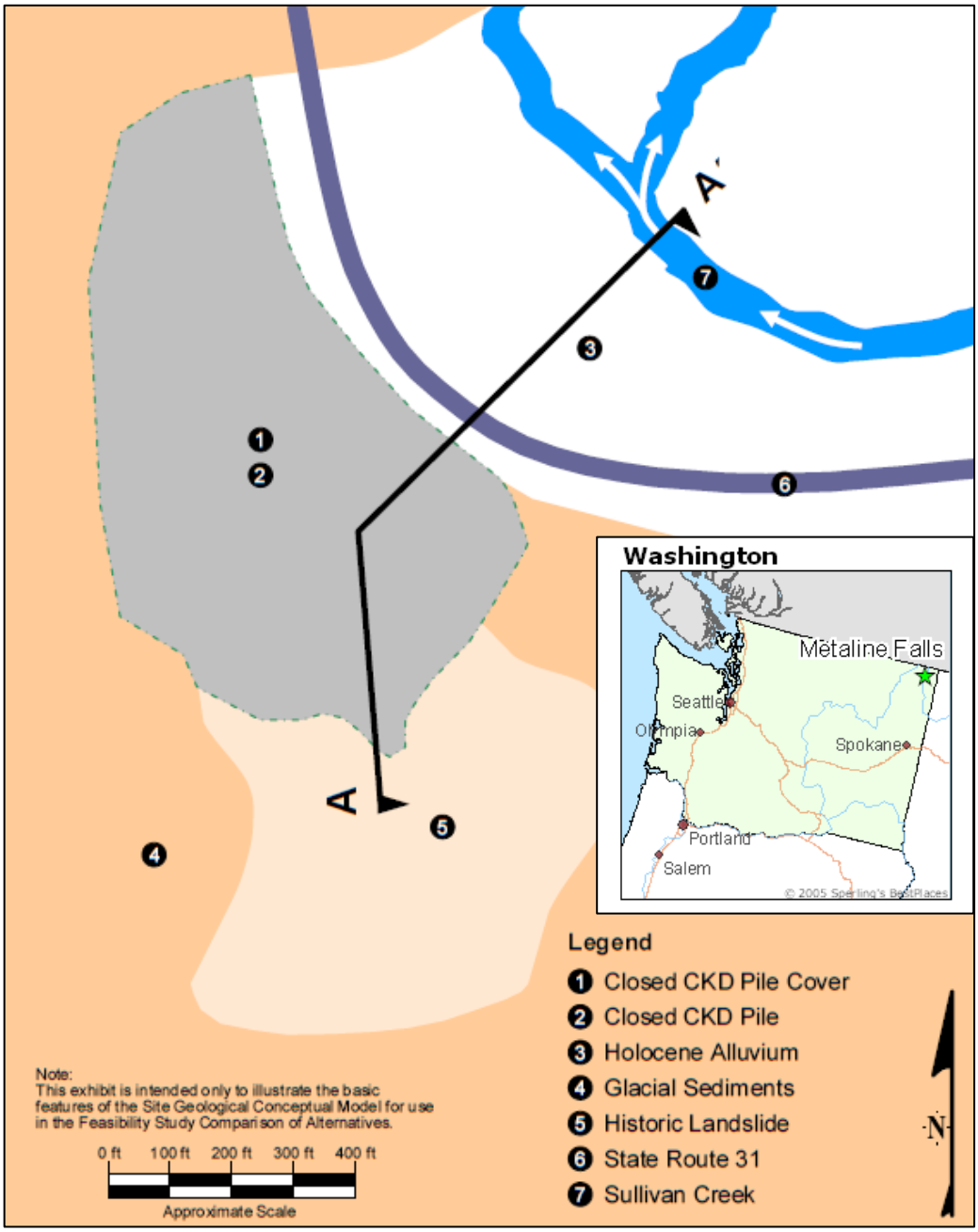

Figure 1: Simplified site map showing the CKD pile in relation to SR 31 and Sullivan Creek, as well as local geologic units. Includes an inset location map of Washington State.

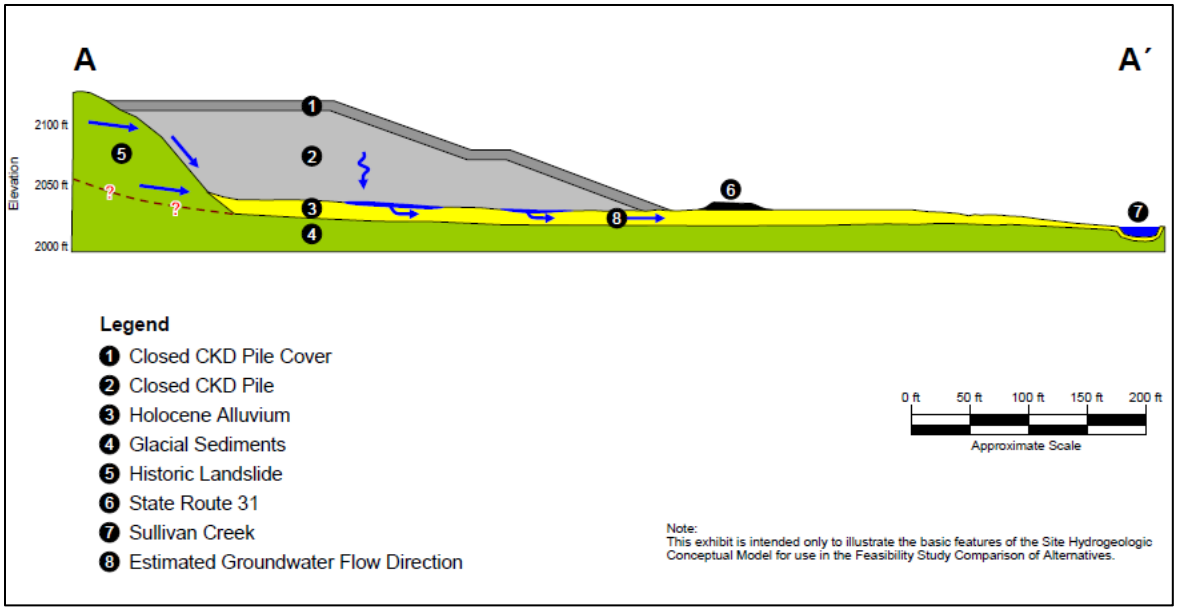

Figure 2: Simplified cross-section of the CKD pile with relative groundwater flow directions. Taken from Geosyntec 2006.

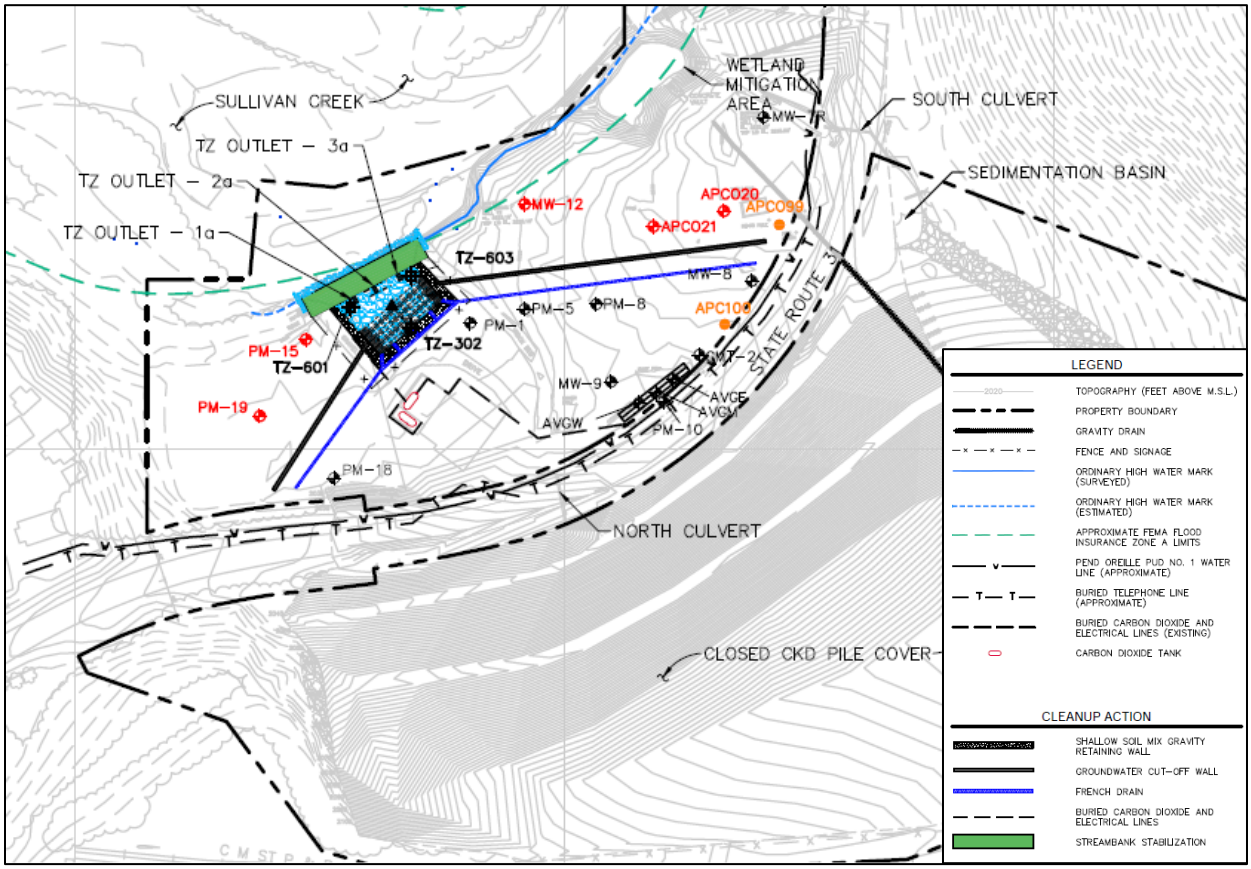

Figure 3: Site map showing treatment cell in relation to the CKD pile and the monitoring wells on site. Taken from Geosyntec 2006.

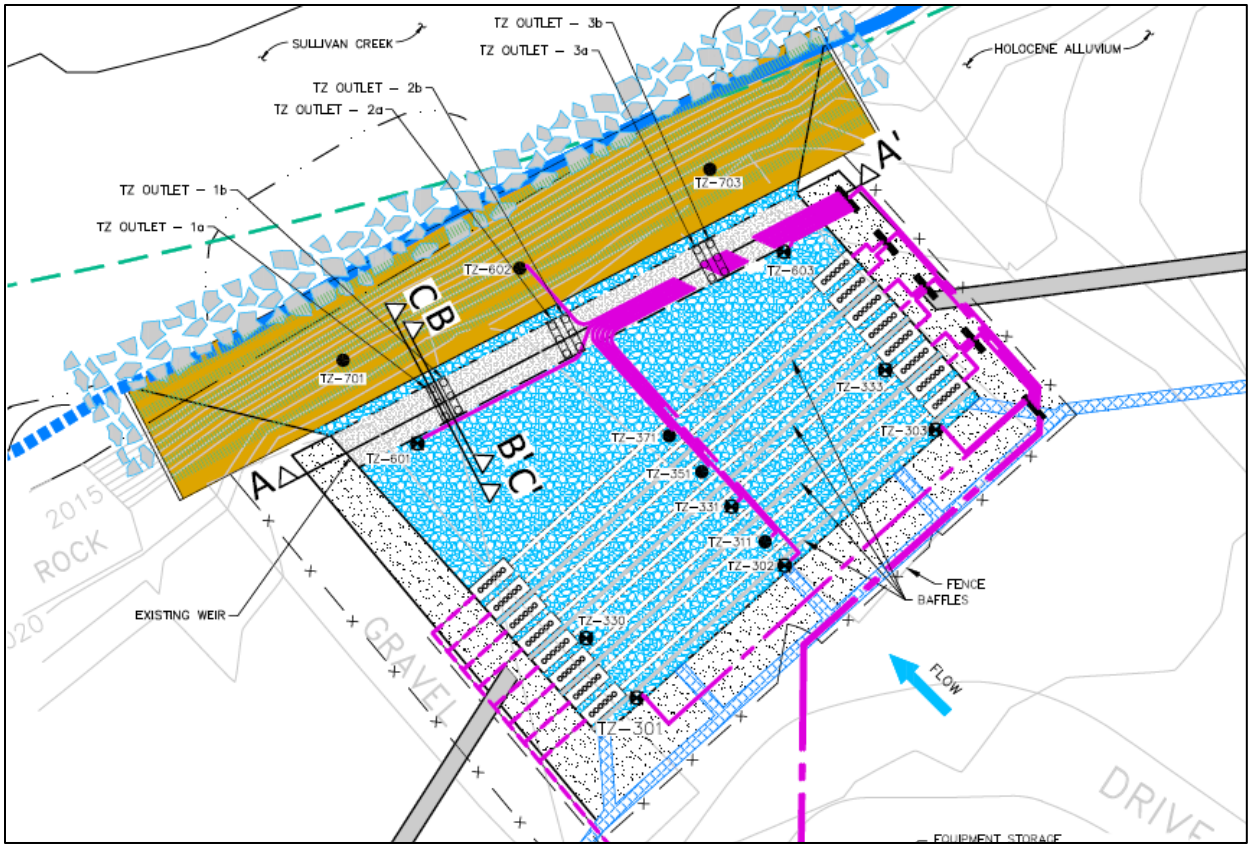

Figure 4: Zoomed in view of the treatment cell. Purple lines are electrical conduit to power the CO_2 injection pumps and recirculation system.

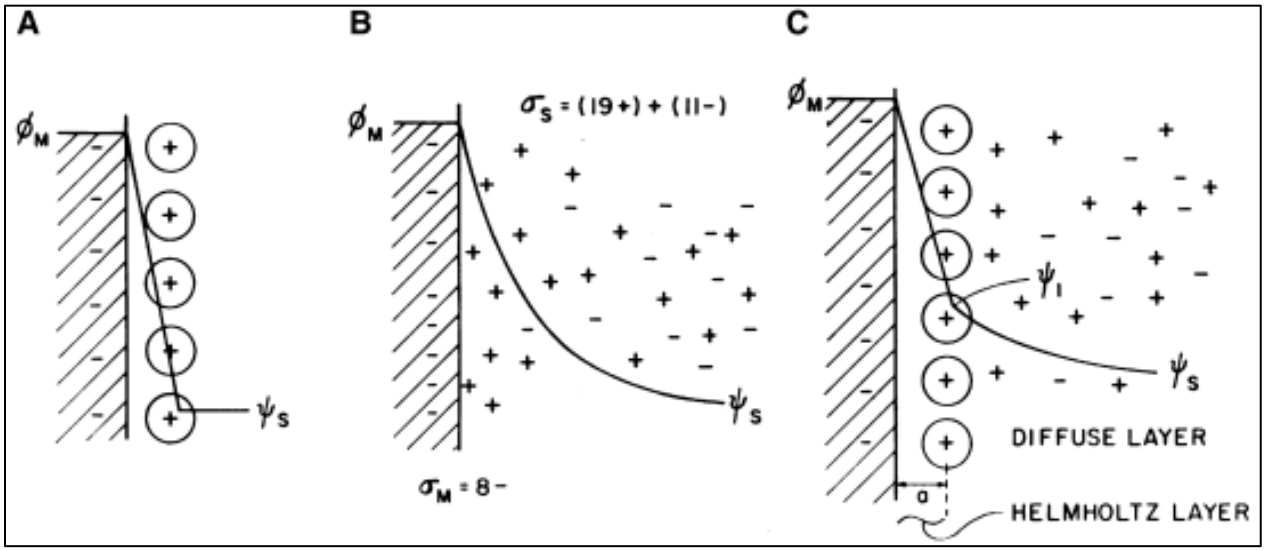

Figure 5: Common electrical surface charge models: (A) the helmholtz model, (B) the Guoy-Chapman model, and (C) the Guoy-Chapman-Stern model. Ψ represents the capacitance or charge as a function of distance from the surface. Figure taken from Wu and Qiao 2014.

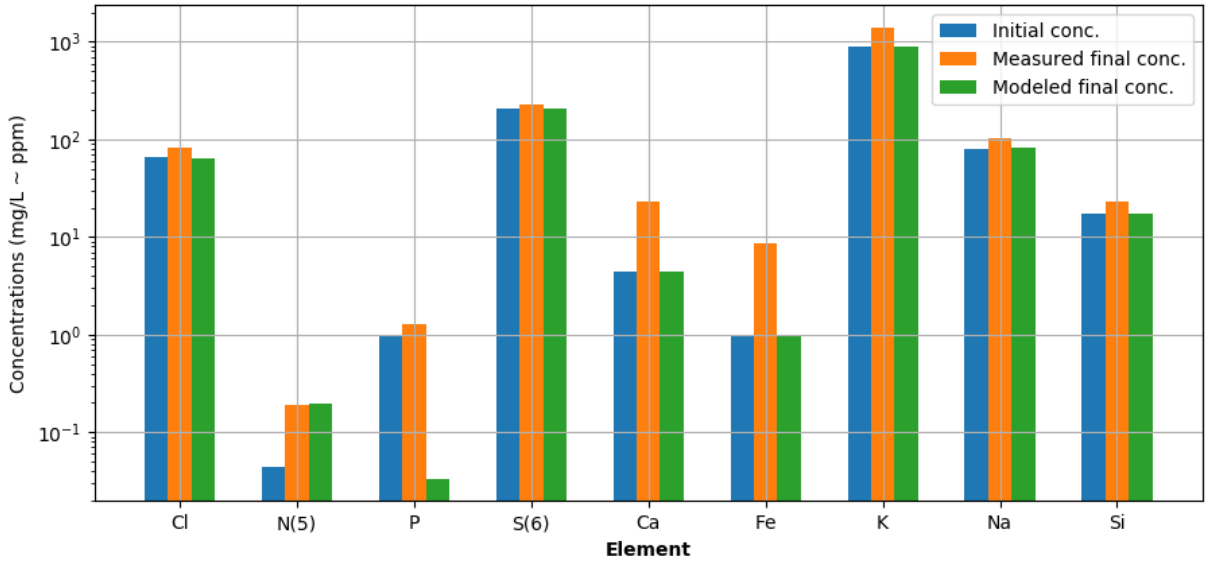

Figure 6: Model validation comparing ion concentrations predicted by Phreeq-C to the measured ion concentrations in the treatment cell. Discrepancies between model predictions and measured final concentrations are most likely due to the fact that PHREEQ-C reports equilibrium concentrations, while conditions inside the treatment cell are still equilibrating.

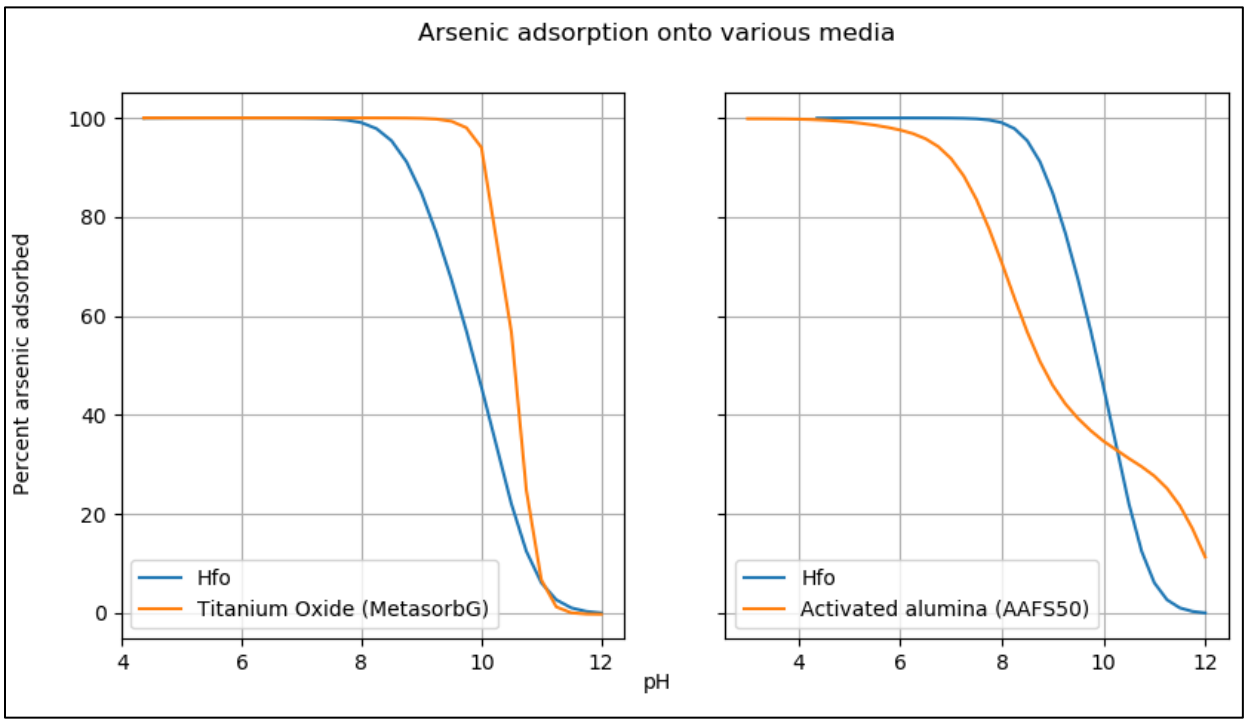

Figure 7: Model predictions of arsenic adsorption between hydrous ferric oxide (Hfo) and titanium oxide and activated alumina. Trials were run without other ions present (i.e. just the media and arsenic). MetasorbG performs better than Hfo, while AAFS50 performs worse.

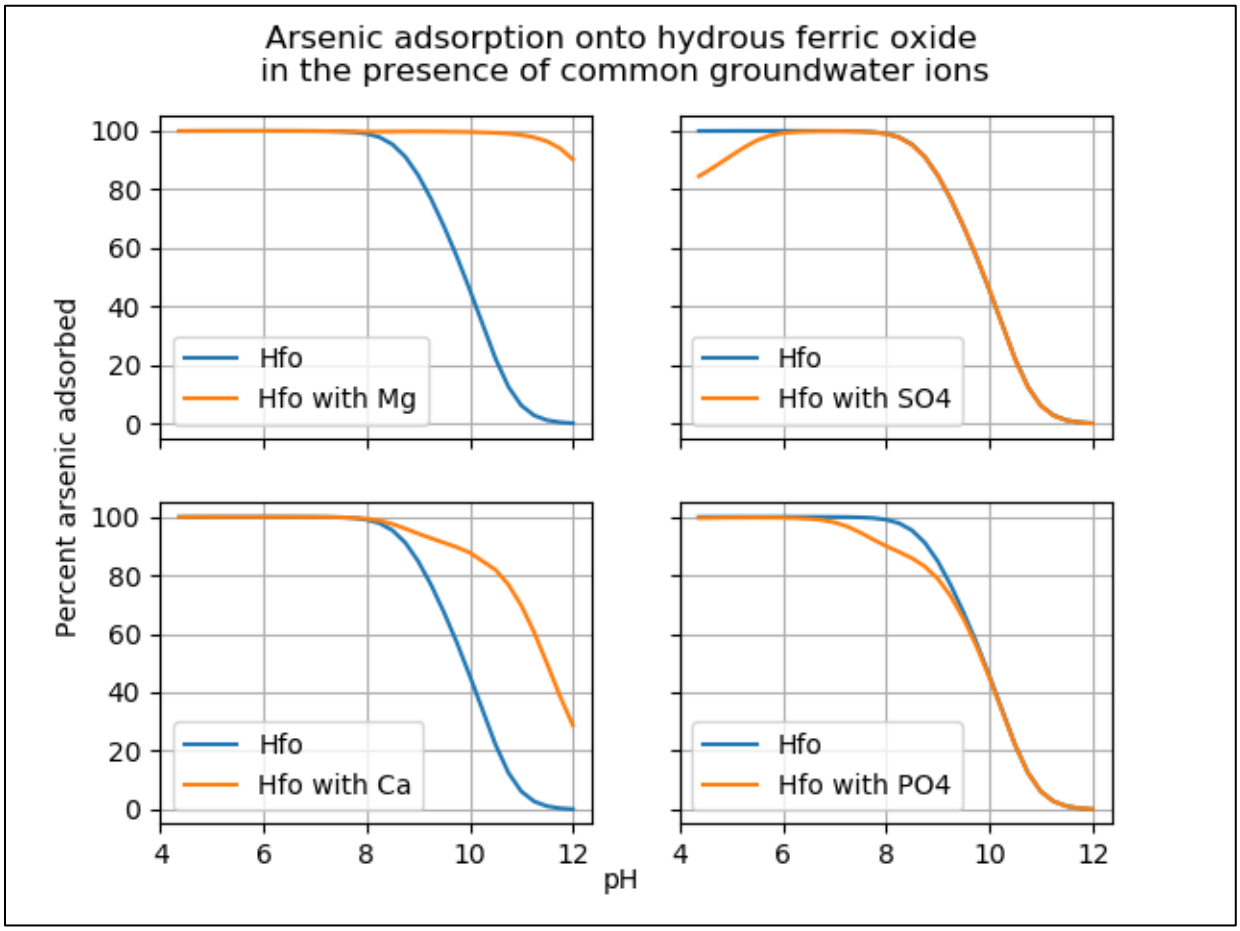

Figure 8: Model predictions of effects on arsenic adsorption by various ions. Trials were run with only arsenic and the desired ions present (i.e. low ionic strength). Cations encourage arsenic adsorption above the pH_{ZC} while anions inhibit arsenic adsorption below the pH_{ZC}.

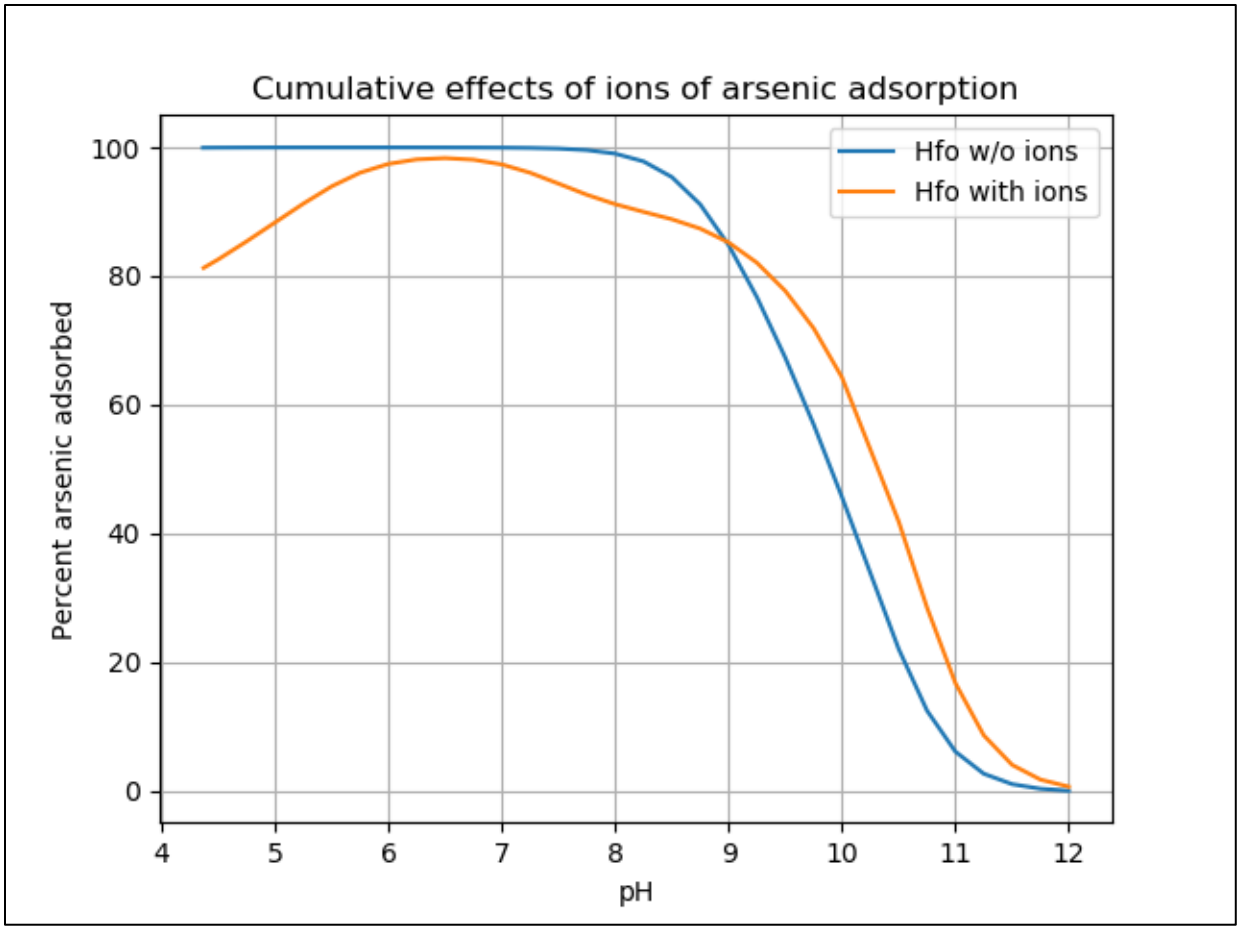

Figure 9: Comparing arsenic adsorption onto hydrous ferric oxide (Hfo) between an arsenic-only solution and in-situ conditions. This figure illustrates the cumulative effects of both anions and cations on arsenic adsorption.

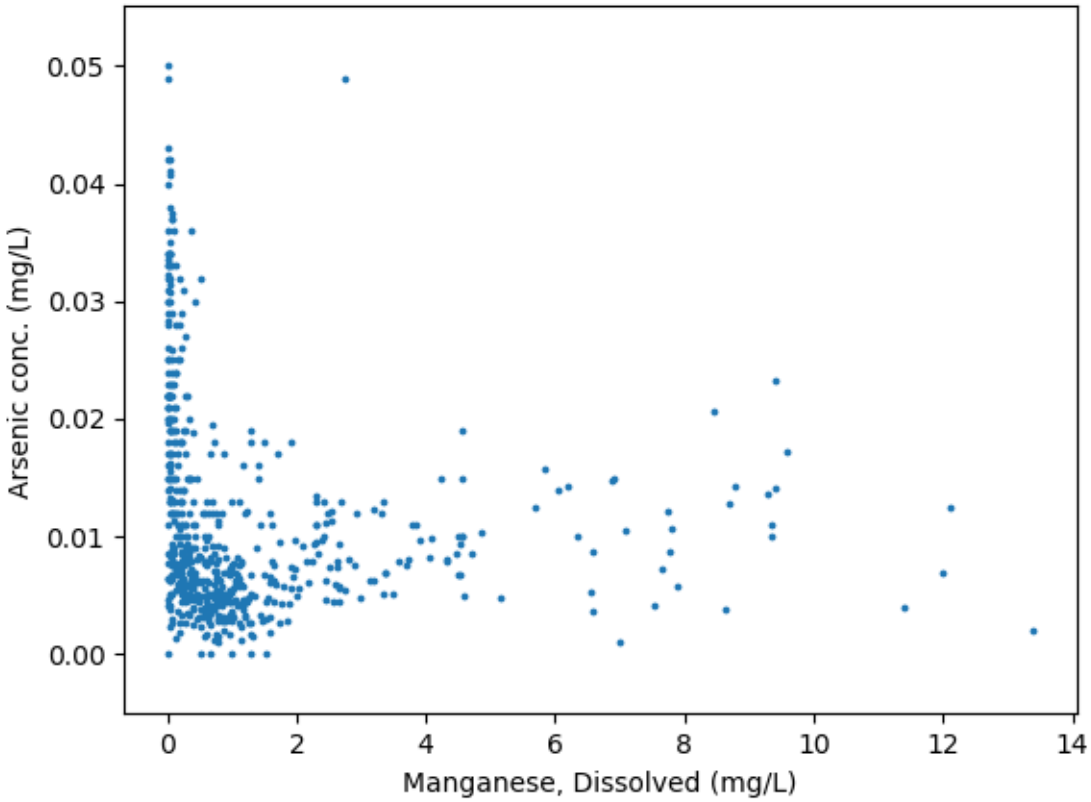

Figure 10: Scatter plot showing the relationship between manganese and arsenic concentration. While not having a strong correlation coefficient, it is evident that there are either high levels of manganese or arsenic in the treatment cell, but never both.

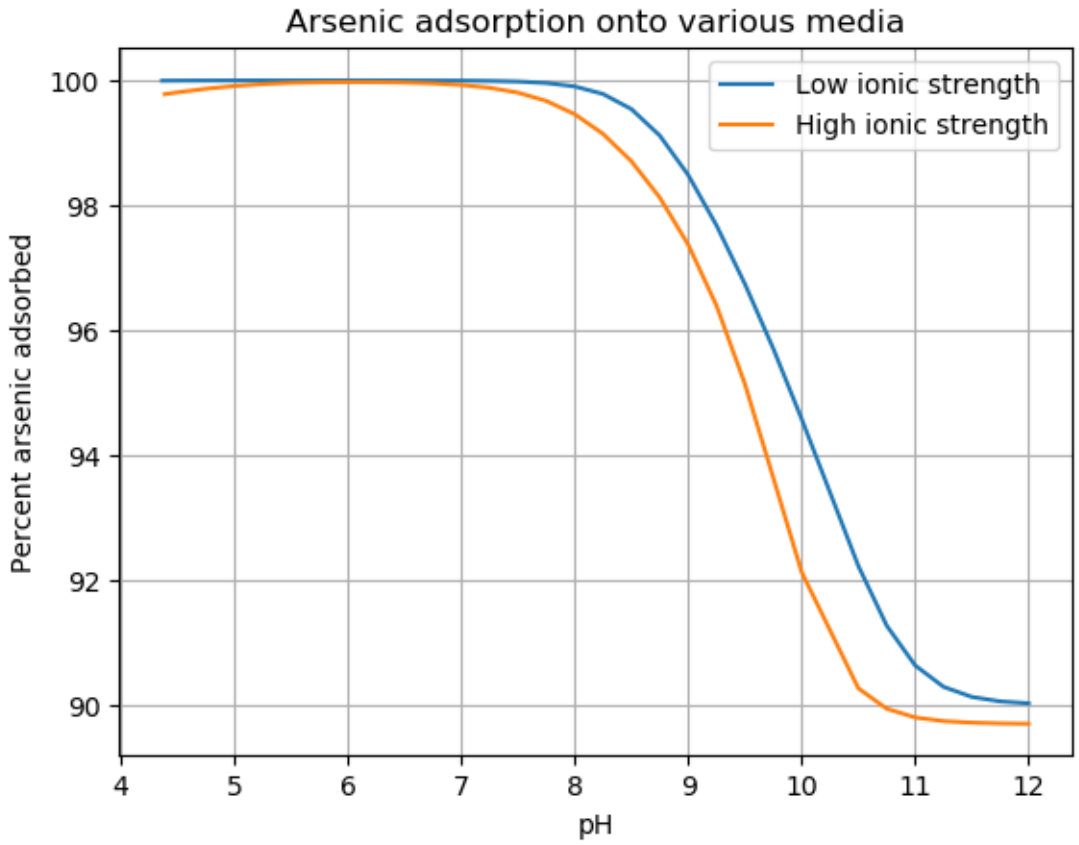

Figure 11: Comparing arsenic adsorption to Hfo under low ionic strength (I = 0.06 mol/kg) and high ionic strength (I = 0.49 mol/kg). Ionic strength was adjusted using a balanced ratio of chlorine and potassium to maintain a neutral solution charge. Cl and K were chosen because they were shown to not interact with the Hfo surface or arsenic in solution in the model trials.

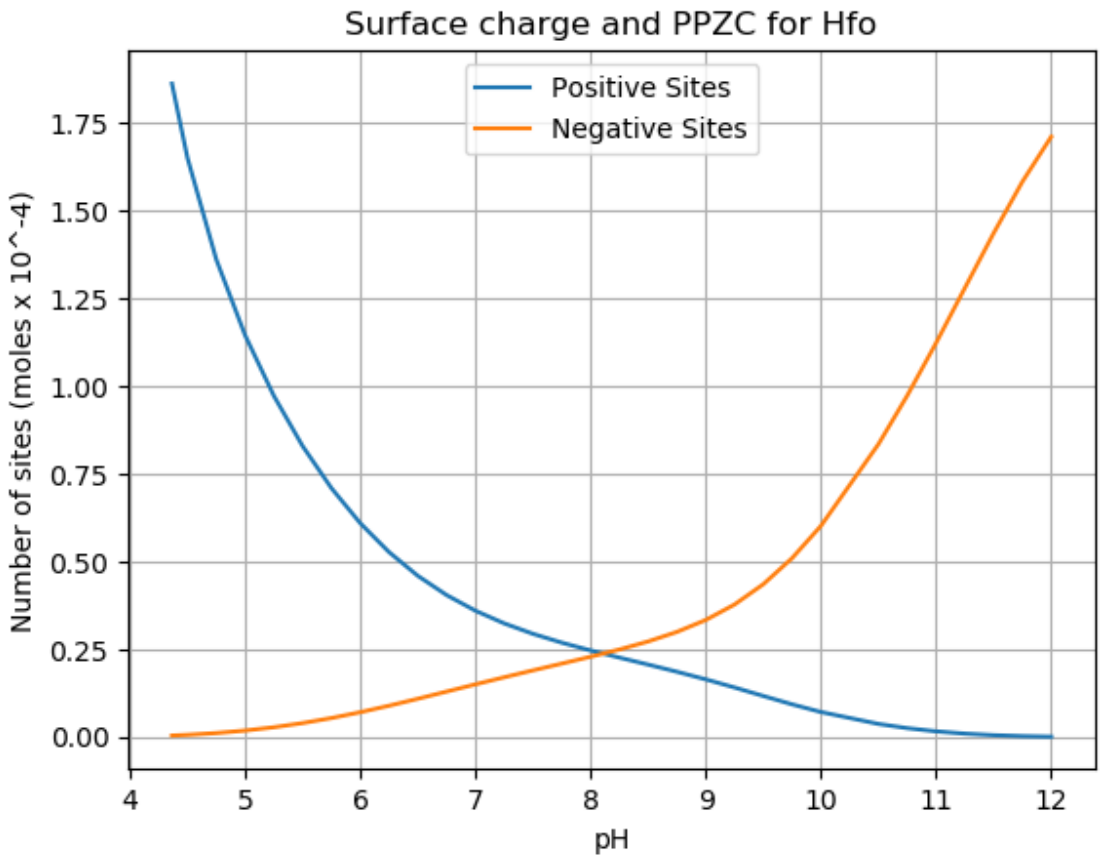

Figure 12: Plot of the total number of positive and negative surface sites for Hfo. This graph shows the "pristine" point-of-zero-charge at pH = 8.1, where the number of positive and negative sites are equal. Pristine point-of-zero-charge refers to the pH_{ZC} when the only ions present are hydrogen ions and hydroxide ions.

	Arsenic	Chromium	Cond	DO	Lead	Manganese	ORP	Temp	Turb	pH
Arsenic	1									
Chromium	0.395375	1								
Cond	0.674437	0.45798	1							
DO	0.042864	0.0134445	-0.07247	1						
Lead	0.371134	0.186334	0.188893	0.155657	1					
Manganese	-0.15016	-0.146915	-0.11942	-0.10174	-0.18969	1				
ORP	-0.30508	-0.100843	-0.34322	0.120315	-0.10783	0.104124	1			
Temp	0.079421	0.0101311	-0.064	0.051025	0.082566	0.118842	-0.015	1		
Turb	0.064768	0.0132523	0.056335	0.186376	0.006877	-0.0341422	-0.04138	-0.02017	1	
pH	0.548341	0.180719	0.414161	0.036094	0.347237	-0.484943	-0.47916	-0.15688	0.115242	1

Table 1: Correlation matrix showing the Pearson's correlation coefficient between each variable. The highlighted variables (conductivity, oxidation-reduction potential, and pH) have the largest influence on arsenic levels.

sample ID	Cl	NO3-N	PO4-P	SO4-S	Al	As	B	Ba	Ca	Cd	Cr	Cu	Fe
	mg/L	mg/L	mg/L	mg/L	mg/L	mg/L	mg/L	mg/L	mg/L	mg/L	mg/L	mg/L	mg/L
TZ-01	31.9	0.052	0.284	82.7	TR	TR	ND	ND	7.02	ND	ND	ND	2.74
Re-circ	31.6	0.039	0.25	91.1	ND	TR	ND	TR	7.43	ND	ND	ND	4.3
TZ-03	19.5	0.099	0.752	54.9	ND	ND	ND	ND	8.8	ND	ND	ND	1.5
PM-5	104	0.05	0.135	139	TR	TR	TR	ND	4.16	ND	ND	ND	0.72
MW-9	43.04	0.053	1.237	298	0.82188	ND	ND	ND	1.44	ND	ND	ND	0.92
PM-1	51.9	0.029	1.642	191	TR	TR	ND	ND	7.84	ND	ND	ND	1.35
QC run	1.08	1.03	1.08	1.11	24.86	5.12129	4.91	4.94	24.5	4.91	4.98	4.94	4.88
QC true	1.00	1.00	1.00	1.00	25.00	5.00	5.00	5.00	25.00	5.00	5.00	5.00	5.00

sample ID	K	Mg	Mn	Mo	Na	Ni	P	Pb	S	Se	Zn	Si	Ag
	mg/L	mg/L	mg/L	mg/L	mg/L	mg/L	mg/L	mg/L	mg/L	mg/L	mg/L	mg/L	mg/L
TZ-01	472.7	TR	0.33678	TR	36.5	ND	TR	ND	67.8	ND	ND	7.61	ND
Re-circ	570.1	TR	0.43392	ND	40.6	ND	TR	ND	80.2	ND	ND	10.4	ND
TZ-03	347.3	TR	0.24294	ND	27	ND	TR	ND	47.6	ND	ND	5.04	ND
PM-5	461.3	4.3965	ND	TR	106	ND	ND	ND	121	ND	ND	5.76	ND
MW-9	1503	TR	ND	0.6135	77.9	ND	TR	ND	259	ND	ND	38.8	ND
PM-1	687	7.17666	TR	TR	58.9	ND	TR	ND	131	ND	ND	6.8	ND
QC run	48.06	4.80	4.90688	4.93957	9.73	4.91	10.2	4.97	4.95	4.86	4.91	4.93	4.89
QC true	50.00	5.00	5.00	5.00	10.00	5.00	10.00	5.00	5.00	5.00	5.00	5.00	5.00

Table 2: ICP-MS lab results from the field samples.

	PM-1	MW-9	PM-5	TZ-01	TZ-03	Recirc
Time of data collection	9:45 AM	10:30 AM	11:35 AM	1:00 PM	1:45 PM	N/A
Depth to water (ft)	4.07	3.71	5.48	N/A	N/A	N/A
Depth of well (ft)	18.01	15.78	17.13	N/A	N/A	N/A
Tubing depth (ft)	11	9.75	11.3	N/A	N/A	N/A
Temperature (Celsius)	14.93	20.86	16.59	18.24	17.27	N/A
pH	10.48	11.61	10.07	7.21	7.08	N/A
ORP (mV)	-222	-238	-226	-96	-229	N/A
Conductivity (mS/cm)	2.56	4.76	2.14	1.76	1.37	N/A
NTU	2.9	6.3	0.5	0	0.9	N/A
DO (mg/L)	1.31	1.45	0.85	0.97	0.89	N/A
TDS (g/L)	1.64	3.06	1.37	1.13	0.873	N/A

Table 3: Water quality parameters taken when groundwater samples were collected.

7.0 References

Azam, M.S., Shafiquzzaman, M., Nakajima, J., 2010, Effect of Calcium and Magnesium Addition on Arsenic Leaching from Paddy Field Soil of Bangladesh, Journal of Water and Environmental Technology, v. 8, p 329-338, doi: 10.2965/jwet.2010.329.

Bowell, R. J., Alpers, C. N., Jamieson, H. E., Nordstrom, D. K., Majzlan, J., 2014, Environmental Geochemistry, Mineralogy, Microbiology of Arsenic: Mineralogical Society of America, Reviews in Mineralogy and Geochemistry ; v. 79.

Dai, M., Xia, L., Song, S., Peng, C., and Lopez-Valdivieso, A., 2016, Adsorption of As(V) inside the pores of porous hematite in water: Journal of Hazardous Materials, v. 307, p. 312–317, doi:10.1016/j.jhazmat.2016.01.008.

Davies, J.A., and Kent, D.B., 1990, Surface Complexation Modeling in Aqueous Geochemistry: Mineralogical Society of America, Reviews in Mineralogy and Geochemistry ; v. 23, p. 177-260.

Dzombak, D., and Morel, F., 1990, Surface Complexation Modeling: Hydrous Ferric Oxide: 416 p., https://www.wiley.com/en-us/Surface+Complexation+Modeling%3A+Hydrous+Ferric+Oxide-p-9780471637318 (accessed January 2020).

Environmental Protection Agency (EPA), 2000, Technologies and Cost for Removal of Arsenic from Drinking Water.

Geosyntec Consultants (Geosyntec), 2006, Engineering Design Report: [Redacted] Company Closed Cement Kiln Dust Site, Metaline Falls, Washington.

Goldberg - (1986) Chemical Modeling of Arsenate Adsorption on.pdf, https://www.ars.usda.gov/arsuserfiles/20360500/pdf_pubs/P0931.pdf (accessed November 2019).

Han, D.S., Abdel-Wahab, A., and Batchelor, B., 2010, Surface complexation modeling of arsenic(III) and arsenic(V) adsorption onto nanoporous titania adsorbents (NTAs): Journal of Colloid and Interface Science, v. 348, p. 591–599, doi:10.1016/j.jcis.2010.04.088.

Hsia, T.-H., Lo, S.-L., Lin, C.-F., and Lee, D.-Y., 1994, Characterization of arsenate adsorption on hydrous iron oxide using chemical and physical methods: Colloids and Surfaces A: Physicochemical and Engineering Aspects, v. 85, p. 1–7, doi:10.1016/0927-7757(94)02752-8.

Kanematsu, M., Young, T.M., Fukushi, K., Green, P.G., and Darby, J.L., 2013, Arsenic(III, V) adsorption on a goethite-based adsorbent in the presence of major co-existing ions: Modeling competitive adsorption consistent with spectroscopic and molecular evidence: Geochimica et Cosmochimica Acta, v. 106, p. 404–428, doi:10.1016/j.gca.2012.09.055.

Parkhurst, D.L., and Appelo, C.A.J., 2013, Description of input and examples for PHREEQC version 3: a computer program for speciation, batch-reaction, one-dimensional transport, and inverse geochemical calculations: U.S. Geological Survey Techniques and Methods USGS Numbered Series 6-A43, 519 p., http://pubs.er.usgs.gov/publication/tm6A43 (accessed January 2020).

Pena, M., Meng, X., Korfiatis, G., and Jing, C., 2006, Adsorption Mechanism of Arsenic on Nanocrystalline Titanium Dioxide: Environmental Science & Technology, v. 40, p. 1257–1262.

Su, T., Guan, X., Gu, G., and Wang, J., 2008, Adsorption characteristics of As(V), Se(IV), and V(V) onto activated alumina: Effects of pH, surface loading, and ionic strength: Journal of Colloid and Interface Science, v. 326, p. 347–353, doi:10.1016/j.jcis.2008.07.026.

Sverjensky, D.A., and Fukushi, K., 2006, A predictive model (ETLM) for As(III) adsorption and surface speciation on oxides consistent with spectroscopic data: Geochimica et Cosmochimica Acta, v. 70, p. 3778–3802, doi:10.1016/j.gca.2006.05.012.

Tournassat, C., Charlet, L., Bosbach, D., and Manceau, A., 2002, Arsenic(III) Oxidation by Birnessite and Precipitation of Manganese(II) Arsenate: Environmental Science & Technology, v. 36, p. 493–500, doi:10.1021/es0109500.

Wilkie, J.A., and Hering, J.G., 1996, Adsorption of arsenic onto hydrous ferric oxide: effects of adsorbate/adsorbent ratios and co-occurring solutes: Colloids and Surfaces A: Physicochemical and Engineering Aspects, v. 107, p. 97–110, doi:10.1016/0927-7757(95)03368-8.

Wu, P., and Qiao, R., 2014, Concept of double layers - Physics and Applications of Double Layers in Ionic Liquids: Clemson University, https://sites.google.com/a/g.clemson.edu/ionic-liquids/home/concept-of-double-layers (accessed January 2020).

Zhang, G., Liu, F., Liu, H., Qu, J., and Liu, R., 2014, Respective Role of Fe and Mn Oxide Contents for Arsenic Sorption in Iron and Manganese Binary Oxide: An X-ray Absorption Spectroscopy Investigation: Environmental Science & Technology, v. 48, p. 10316–10322, doi:10.1021/es501527c.

Zhang, Y., Zhu, C., Liu, F., Yuan, Y., Wu, H., and Li, A., 2019, Effects of ionic strength on removal of toxic pollutants from aqueous media with multifarious adsorbents: A review: Science of The Total Environment, v. 646, p. 265–279, doi:10.1016/j.scitotenv.2018.07.279.

9.0 Acknowledgements

Thanks Adriana Jarosz and Michelle Myers for providing the data and giving guidance through the scoping process. Thanks to Frank for helping me collect samples in the field. Thanks to Drew for helping me navigate PHREEQ-C and providing insight into all things geochemistry. Thanks to Michael Brown for editing and reviewing the paper. And thanks to Kathy Troost and MESSAGe cohort 7 for the support and editing.

10.0 Appendices

10.1 Python script

####The following script is used for filtering through the field parameters and lab analyses

collected by Geosyntec in order to determine the pearson coefficient###

```
"""
Created on Sat Dec 21 11:08:39 2019

@author: Luke R
"""

import pandas as pd
import numpy as np
import matplotlib.pyplot as plt

#read in excel files and select the columns i want to look at
df = pd.read_csv(r'C:\Users\Charles\Downloads\MF_analytical_data.csv',encoding='latin-
1',dtype='str',skiprows=range(1,13210))
df = df[['LocationName','CustomerSampleNumberOrig','CollectDate','SampleType','Analyte','Result
(original)']]
df = df.loc[df['SampleType'] != 'Duplicate']
df['CustomerSampleNumberOrig'] = df['CustomerSampleNumberOrig'].str.contains('NoDis',case=False)
== True

df2 = pd.read_csv(r'C:\Users\Charles\Downloads\MF_Field_Parameters.csv',encoding='latin-
1',dtype='str',skiprows=[0,1,2])
df2 = df2[['Well','CollectDate','Temp','pH','Cond','DO','ORP','Turb']]
df2.loc[df2['Well'].str.contains('TZOutlet-1'), 'Well'] = 'TZ1'
df2.loc[df2['Well'].str.contains('TZOutlet-2'), 'Well'] = 'TZ2'
df2.loc[df2['Well'].str.contains('TZOutlet-3'), 'Well'] = 'TZ3'

#select raw data by well (need to do each well individually because naming conventions are not consistent
over 20 years...)
TZ1 = df.iloc[:,0].str.contains('TZOutlet1|TZOutlet-1|TZOutlet-01',case=False)
TZ1 = df[TZ1]
TZ2 = df.iloc[:,0].str.contains('TZOutlet2|TZOutlet-2|TZOutlet-02',case=False)
TZ2 = df[TZ2]
TZ3 = df.iloc[:,0].str.contains('TZOutlet3|TZOutlet-3|TZOutlet-03',case=False)
TZ3 = df[TZ3]
TZ302 = df.iloc[:,0].str.contains('TZ-302',case=False)
TZ302 = df[TZ302]
TZ601 = df.iloc[:,0].str.contains('TZ-601',case=False)
TZ601 = df[TZ601]
TZ603 = df.iloc[:,0].str.contains('TZ-603',case=False)
TZ603 = df[TZ603]
PM10 = df[df['LocationName'] == 'PM-10']
PM11 = df[df['LocationName'] == 'PM-11']
PM12 = df[df['LocationName'] == 'PM-12']
```

```
PM13 = df[df['LocationName'] == 'PM-13']
PM14 = df[df['LocationName'] == 'PM-14']
PM15 = df[df['LocationName'] == 'PM-15']
PM16 = df[df['LocationName'] == 'PM-16']
PM17 = df[df['LocationName'] == 'PM-17']
PM18 = df[df['LocationName'] == 'PM-18']
PM19 = df[df['LocationName'] == 'PM-19']
MW12 = df[df['LocationName'] == 'MW12']
MW7 = df[df['LocationName'] == 'MW7']
MW8 = df[df['LocationName'] == 'MW8']
MW9 = df[df['LocationName'] == 'MW9']


#create lists and dict for looping through wells and analytes
labvariables = ['pH','Arsenic, Dissolved','Chromium, Dissolved','Lead, Dissolved','Manganese,
Dissolved']
fieldparam = ['Temp','Cond','DO','ORP','Turb']
d = {} #dict to hold filtered data
wells =
[TZ1,TZ2,TZ3,TZ302,TZ601,TZ603,PM10,PM11,PM12,PM13,PM14,PM15,PM16,PM17,PM18,PM19,
MW7,MW8,MW9,MW12] # raw data by well
wellnames = ['TZ1','TZ2','TZ3','TZ-302','TZ-601','TZ-603','PM-10','PM-11','PM-12','PM-13','PM-
14','PM-15','PM-16','PM-17','PM-18','PM-19','MW7','MW8','MW9','MW12'] #list of well names for
naming in loop

#loop through the raw data for each well and add each analyte to the dataframe and then add all analytes
to dict (d)
for i,w in enumerate(wells):
    d['well{0}'.format(i)] = pd.DataFrame(columns=range(0,2))
    d['well{0}'.format(i)].columns = ['Location','CollectDate']
    for v in labvariables:
        a = w.loc[w['Analyte']==v][['CollectDate','Result (original)']]
        a = a.drop_duplicates(subset='CollectDate')
        d['well{0}'.format(i)] = pd.merge(d['well{0}'.format(i)],a,on='CollectDate',how='outer')
        d['well{0}'.format(i)].rename(columns={'Result (original)':v},inplace=True)
    for f in fieldparam:
        a = df2[['Well','CollectDate',f]]
        a = a.loc[a['Well']==wellnames[i]]
        a = a[['CollectDate',f]]
        d['well{0}'.format(i)] = pd.merge(d['well{0}'.format(i)],a,on='CollectDate',how='outer')
    d['well{0}'.format(i)]['Location'] = d['well{0}'.format(i)]['Location'].fillna(wellnames[i])
    #nodis = df[['CollectDate','CustomerSampleNumberOrig']].isin(d['well{0}'.format(i)]['CollectDate'])
    #d['well{0}'.format(i)] = pd.merge(d['well{0}'.format(i)],nodis,on='CollectDate')

#merge all well data into single dataframe and drop any rows with na and replace No Detection with 0
and sort by date
data = pd.concat(d,sort=True)
data = data.reset_index(drop=True)
data = data.dropna()
data = data.replace('ND',0)
data['CollectDate'] = pd.to_datetime(data['CollectDate'])
```

```
data['Arsenic, Dissolved'] = data['Arsenic, Dissolved'].astype(float)
data = data.loc[data['Arsenic, Dissolved']<=0.05]
data = data.sort_values(by='CollectDate')

#create matrix with only variables to find pearson coefficient
X = data.drop(columns=['CollectDate','Location'])

#final correlation coefficient matrix
corr_mat = np.corrcoef(np.array(X.astype(float)).T)
```

10.2 Media reactions database

###The following is a text database for use in Phreeq-C that includes the adsorption reactions between arsenic and titania oxide and activated alumina###

```
#Titania oxide SCM reactions from Pena et al. 2006
      #tabulate surface
      TiOH = TiOH
            log_k 0.0

      #surface protonation equations
       TiOH + H+ = TiOH2+
            log_k 3.8

       TiOH = TiO- + H+
            log_k -7.8

      #arsenic adsorbtion reactions
      TiOH + TiOH + AsO3-3 + 3H+ = (TiO)2AsO- + 2H2O + H+
            log_k 30.0

      TiOH + TiOH + H2AsO3- = Ti2AsO3- + 2H2O
            log_k -2.0

#Activated alumina SCM reactions from Su et al 2008.
      #tabulate surface
      Aa_aOH2+ = Aa_aOH2+
      log_k 0

      Aa_bwOH2+ = Aa_bwOH2+
      log_k 0

      Aa_bsOH2+ = Aa_bsOH2+
      log_k 0

      Aa_cOH2+ = Aa_cOH2+
      log_k 0
```

```
#protonation reactions

Aa_aOH2+ = Aa_aOH + H+
      log_k -3.33

Aa_bwOH2+ = Aa_bwOH + H+
      log_k -6.57

Aa_bsOH2+ = Aa_bsOH + H+
      log_k -6.57

Aa_cOH2+ = Aa_cOH2+
      log_k -10.6

#Arsenic adsorption reactions

Aa_aOH2+ + H2AsO4- = Aa_aH2AsO4 + H2O
      log_k 3.8

 Aa_aOH2+ + HAsO4-2 = Aa_aHAsO4- + H2O
      log_k 5.7

Aa_bwOH2+ + H2AsO4- = Aa_bwH2AsO4 + H2O
      log_k 5.1

Aa_bwOH2+ + HAsO4-2 = Aa_bwHAsO4- + H2O
      log_k 4.4

Aa_bsOH2+ + H2AsO4- = Aa_bsH2AsO4 + H2O
      log_k 8.2

Aa_bsOH2+ + HAsO4-2 = Aa_bsHAsO4- + H2O
      log_k 7.1

Aa_bsOH2+ + AsO4-3 = Aa_bsAsO4-2 + H2O
      log_k 6.6
```